Journal of Alloys and Compounds 526 (2012) 39–44

Contents lists available at SciVerse ScienceDirect

Journal of Alloys and Compounds

journal homepage: www.elsevier.com/locate/jallcom

Fatigue properties of ultra-fine grain Cu–Cr alloy processed by equal-channel angular pressing

Q.J. Wang*, Z.Z. Du, L. Luo, W. Wang

School of Metallurgy Engineering, Xi'an University of Architecture and Technology, Xi'an 710055, PR China

ARTICLE INFO

Article history:
Received 4 June 2008
Received in revised form 17 February 2012
Accepted 17 February 2012
Available online xxx

Keywords:
Metals
Nanofabrications
Scanning and transmission electron microscopy
Strain

ABSTRACT

A precipitation-hardening copper based alloy (Cu–0.6 wt.% Cr) was selected and the ultra-fine grain (UFG) microstructure was obtained by equal channel angular pressing (ECAP). The alloys tensile behaviors and fatigue properties were investigated experimentally, the results indicated that the Cu–Cr alloy processed by ECAP possessed high strength and sufficient ductility and the 12-passes ECAPed sample with UFG under strain controlled fatigue exhibited cyclic softening and lower fatigue limit compared to the unECAPed one. Moreover, the shear bands on the surface of cycled samples were also studied by scanning electron microscopy, the results showed that the oriented distribution of defects along the shear plane in the last ECAP processing was one of the major mechanisms of SBs formation.

1. Introduction

Equal channel angular pressing (ECAP) has been recognized as a promising method for fabrication of large bulk materials with ultra-fine grain (UFG) sizes through severe plastic deformation [1,2]. In most bulk UFG materials with grain size between 0.1 and 1 μm attained by ECAP display a number of attractive physical and mechanical properties such as enhanced strength and relative high ductility. Up to now, most of studies have been carried out mainly on the microstructures evolvement, mechanical properties and strengthening mechanism of UFG materials, including copper and copper based alloy, aluminium and some of its alloys, magnesium alloys, titanium, invar alloy and low carbon steel, prepared by ECAP [3–12]. However, with respect to potential applications of this new class of bulk UFG materials, the cyclic deformation and fatigue behaviour, relative to that of conventional grain size (CG) materials, is of crucial importance. The recent studies on the fatigue of UFG metals prepared by ECAP have shown in several cases that the fatigue strength of UFG materials is enhanced considerably by grain refinement in the high cycle fatigue (HCF) regime compared to CG material. At the same time, the low cycle fatigue (LCF) performance is reduced because of the lower ductility of the UFG material. The lower fatigue resistance of unstable microstructure of UFG metals in the LCF regime has been mainly related to microstructural features like grain coarsening, cyclic softening, strain localization and macroscopic shear banding [13–15].

The precipitation hardened alloys were found to be most responsive to ECAP in terms of structure refinement, strength enhancement, fatigue life and ductility improvement [13]. The cyclic softening behavior is triggered by grain coarsening under cyclic deformation in the ECAPed pure copper [14]. However, the ECAPed Cu–Cr–Zr, Cu–Cr alloys have not revealed any grain coarsening after cyclic deformation because the grain boundary mobility is strongly restricted by precipitates in Refs. [16,17]. De et al. [18] observed a direct evidence of room temperature recrystallization during fatigue in a precipitation hardened UFG aluminum alloy by a comparative study of the surface microstructural changes during fatigue. Hence, it is unclear if the similar mechanism in pure metal is effective in the precipitation hardened materials. The detailed structural investigations before and after fatigue are still required to clarify the nature of mechanism of the cyclic softening behavior. The course of degradation of UFG metals and alloys leading to final fracture is still under discussion.

Cu–Cr alloy is a promising precipitation-hardening material and used widely in the field of trolley wire, electrode and connectors of various microelectronic devices due to its high strength, high electrical, thermal conductivity and excellent fatigue resistance [19,20]. To expand the application extension, it is still necessary to improve the combination properties of Cu–Cr alloy. In this paper, a precipitation-hardening copper based alloy (Cu–0.6 wt.% Cr) was selected and the microstructure of UFG material processed by ECAP was analyzed. The alloy's tensile behaviors and fatigue properties,

* Corresponding author. Tel.: +86 29 82202821; fax: +86 29 82202706.
E-mail address: jiandawqj@yahoo.com.cn (Q.J. Wang).

0925-8388/$ – see front matter © 2012 Elsevier B.V. All rights reserved.
doi:10.1016/j.jallcom.2012.02.102

including cyclic softening and fracture surface morphology, were investigated experimentally.

2. Experimental procedures

Billets of square 14.5 mm × 14.5 mm cross-section and length of 90 mm of extruded Cu–0.6 wt.% Cr alloy was selected in our experimental studies. The raw material was solid-solution treated at 1293 K for 0.5 h and then quenched into room-temperature water. The quenched billets were followed by aging treatment at 753 K. After aging treatment, the samples were subjected to multiple pressing through an ECAP die having two square channels intersecting at 90°. All of the experiments were performed with the press speed of 2 mm/s at room temperature via the so-called "route C", when the sample was rotated through 180° about working axis between subsequent passes. The pressing strain ε is about 1 for each cycle ECAP pass [21].

The samples for testing were shaped by spark erosion to prepare a specimen with the gauge length of 10 mm and a square cross-section of 4 mm × 4 mm. As shown in Fig. 1, the axis of the specimen was aligned with the direction of extrusion. The strain controlled fatigue experiments were carried out on a hydraulic servo-electric load frame at loading frequency of 0.5 Hz. Tests were performed by strain control under fully reversed tension/compression at constant plastic strain amplitudes, $\varepsilon_{pl} = \Delta\varepsilon_{pl}/2$, ranged from 2×10^{-4} to 10^{-2} at room temperature in air. The tensile tests were conducted on the same testing machine at a constant strain rate of 1 mm/min. The microstructure of the pre-ECAP samples was examined by optical microscopy. A transmission electron microscope (TEM, JEOL 200CX) was employed for microstructure characterization of the as-pressed samples. Thin foils for TEM observation were prepared by a twin-jet polishing technique using a mixture of 33 vol% nitric acid and 67 vol% methanol. The scanning electron microscopy (SEM, FEI Quanta 200) was employed for observation of surface morphologies after fatigue.

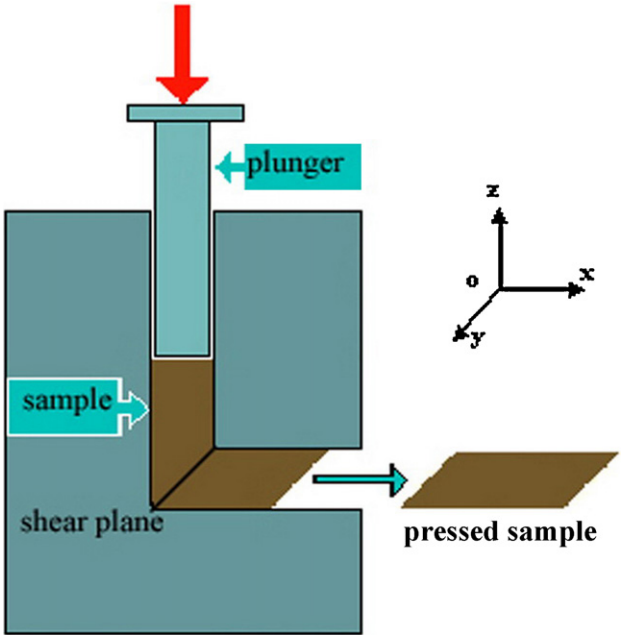

Fig. 1. Illustration of the orientation of the pressed sample and shear plane of the last ECAP pressing.

3. Results and discussion

3.1. Microstructure

Fig. 2 shows the optical photographs of the un-ECAP Cu–0.6 wt.% Cr alloy and TEM micrographs with selected-area electron diffraction (SAED) of the Cu–Cr alloys after different passes of ECAP, respectively. From Fig. 2(a), it can be seen that the microstructure of un-ECAP sample takes on near full equiaxial grain morphology and the average grain size is about 30 μm. The grain boundaries are very clear and there are very few dislocations in the microstructure.

Fig. 2(b) shows a typical microstructure of Cr–Cr after 1 ECA-passes together with a SAED pattern. The thin foil was sectioned from the plane perpendicular to the working axis. The microstructure mainly consists of deformed grains with dense dislocation walls and the average grain size is about length of several microns and width of 0.6 μm. The corresponding SAED shows scattered spots, indicating that the area has low-angle boundaries. The structure of the Cu–Cr alloy subjected to 6 ECA-passes is better seen in the TEM images of Fig. 2(c), showing the fine, nearly equiaxed

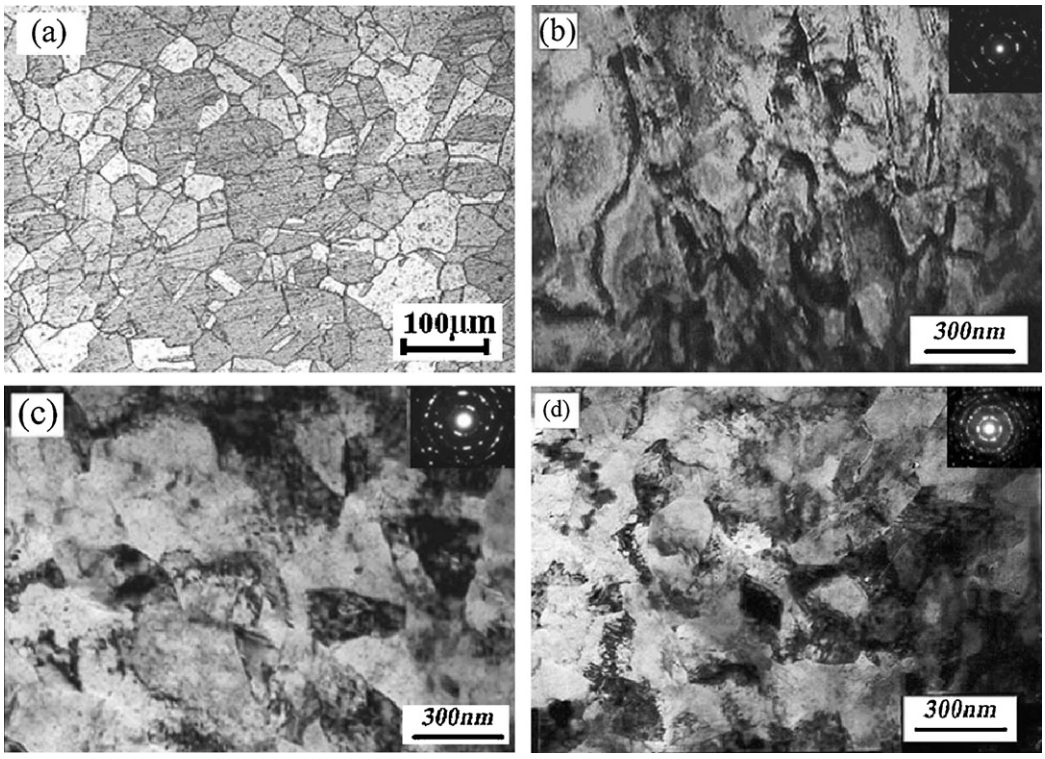

Fig. 2. Optical photographs of the un-ECAP (a) and the typical microstructure of Cu–Cr alloy after different passes: (b) 1 pass; (c) 6 passes; (d) 12 passes.

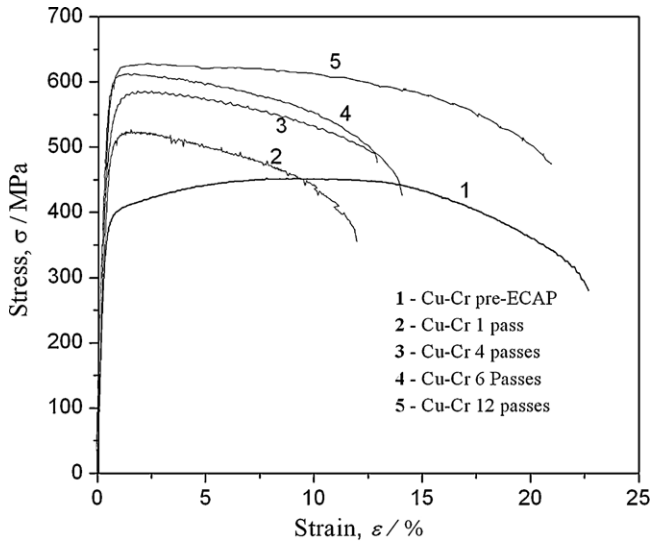

Fig. 3. Tensile stress–strain curves for ECAPed and pre-ECAPed the Cu–Cr alloy.

subgrains, with high dislocation densities both at grain boundaries and inside grains. The SAED pattern is a diffused ring-like pattern with extra spots, indicating that the ultrafine grain structure with high-angle boundaries is generated. The grain size after 12 ECA-passes is nearly 230 nm in average as evaluated from TEM micrographs by the intercept method in the as-fabricated state. In Fig. 2(d), the SAED pattern shows a more uniformly continuous distribution of diffraction images as compared with Fig. 2(b) and (c). The SAED pattern consists of rings of diffraction spots demonstrating that the grain boundaries have high angles of misorientation and the microstructures become more homogeneous and refinement with the increase of the processing passes.

3.2. Tensile behavior

The tensile stress–strain curves of the alloy samples prepared by the ECAP with different numbers of passes are shown in Fig. 3, in which the curve of No. 1 denoted the stress–strain relation for the common un-ECAP alloy sample. Data for yield stress (YS), ultimate tensile strength (UTS), and elongation to failure are summarized in Fig. 4. From Figs. 3 and 4, it can be seen that both

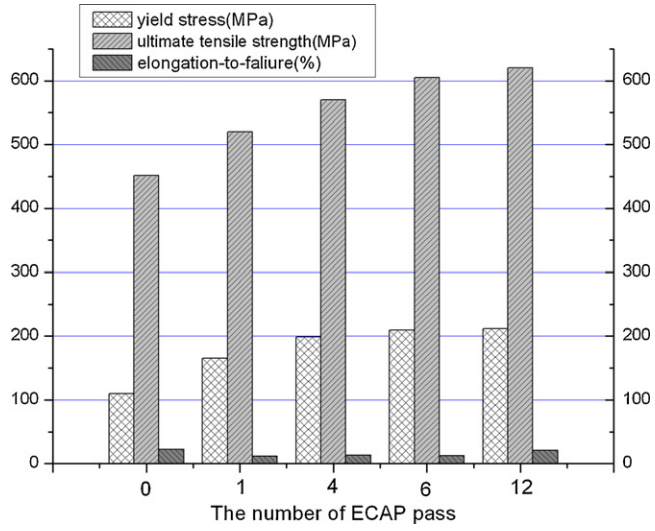

Fig. 4. Yield stress, ultimate tensile strength and elongation-to-failure of the tensile specimens in different conditions.

yield stress and maximum stress increase with the increasing number of ECAP passes. ECAP specimens after 6 and 12 passes, their ultimate tensile strength increase to 605 ± 15 and 620 ± 10 MPa correspondingly and become much higher than pre-ECAPed sample ($\sigma_{UTS} = 451 \pm 10$ MPa). The stress–strain curves as shown in Fig. 3 indicate that the hardening rate of the alloy increases significantly after the process of ECAP. Therefore, the criterion for necking is fulfilled at relatively small strains and uniform elongation decreases.

Moreover, it can be found an interesting phenomenon about the evolution of elongation-to-failure: in contrast to the case of CG alloy, the elongation-to-failure after one pass of ECAP first decreases from 22% to 11.7% greatly, but it subsequently increases with the increasing number of passes. The elongation-to-failure of the alloy sample after finishing 12 passes of ECAP, as denoted with the curve of No. 5 in Fig. 3, is much larger than those of 1, 4 and 6 passes of ECAP. The result is in accordance with Ref. [22]. The cause that strength increases while elongation-to-failure decreases after finishing the first pass of ECAP is ascribed to the formation of great internal stress and high density dislocations induced by the severe plastic strain during ECAP. The elongation-to-failure can be increased pass by pass in concert with the improvement of strength during the following ECAP process. The characteristics of microstructure evolution, such as the grains are refined gradually, and its homogeneity are improved as well as the misorientations are increased with the increasing number of ECAP passes, can all promote plasticity to certain extent [23]. It implies that the homogeneous refinement of the grain structure would lead to a better ductility in metals. As a result, the plasticity of materials at room temperature could be improved pass by pass.

3.3. Fatigue properties

The results of LCF are important for better understanding the mechanisms of plastic deformation in general and of fatigue in particular. The empirical relationship between the plastic strain and the fatigue lifetime can be described as called Coffin–Manson relationship, the plastic deformation is expressed as:

$$\frac{\Delta\varepsilon_p}{2} = \varepsilon_f'(2N_f)^c$$

where $\Delta\varepsilon_p/2$ is the plastic strain amplitude, ε_f' is the fatigue-ductility coefficient, $2N_f$ is the number of reversals to failure and c is the fatigue-ductility exponent. The plastic strain component is dominant and the fatigue life is determined by ductility. Concerning the LCF Coffin–Manson data of strain controlled fatigue tested for the Cu–Cr alloy are shown in Fig. 5. One can see that the fatigue resistance of the pre-ECAP Cu–Cr alloy is superior to that of the UFG Cu–Cr alloy in the 12-pass ECAP state. The best straight line fit for the Coffin–Manson plot is obtained by linear regression analysis. As shown in Fig. 5, Coffin–Manson lines reveal that the values of ε_f' and c are both notably different between the CG Cu–Cr alloy and the UFG Cu–Cr alloy. Their Coffin–Manson curves can be described by the following equations:

$$\frac{\Delta\varepsilon_p}{2} = 1.091(2N_f)^{-0.776} \quad \text{for pre-ECAPed specimens;}$$

$$\frac{\Delta\varepsilon_p}{2} = 0.341(2N_f)^{-0.924} \quad \text{for ECAPed specimens.}$$

It is worth noting, that the slope of the Coffin–Manson line is higher for the ECAP specimens ($c = -0.924$) than the CG copper ($c = -0.776$). There is obvious relation between fatigue lifetime and tensile properties. Comparing with the coarse grain (CG) Cu–Cr alloy (pre-ECAP) with a low strength, the UFG counterpart takes on a higher tensile strength but a lower ductility, and the strain-controlled cyclic properties are also poorer. The plastic strain

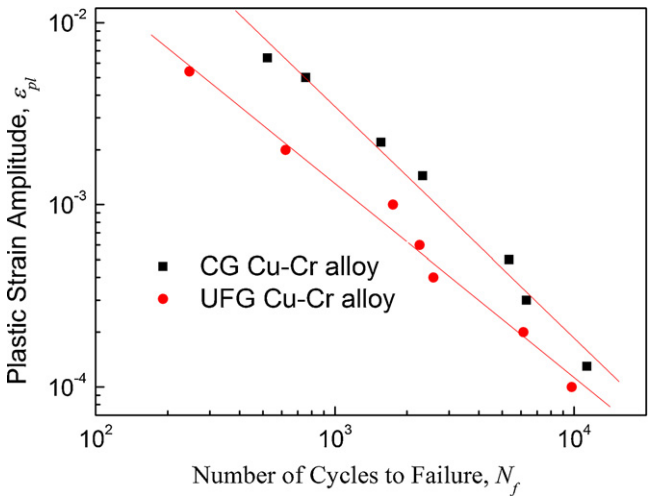

Fig. 5. Coffin–Manson plot of the UFG and CG Cu–0.6 wt.% Cr alloy.

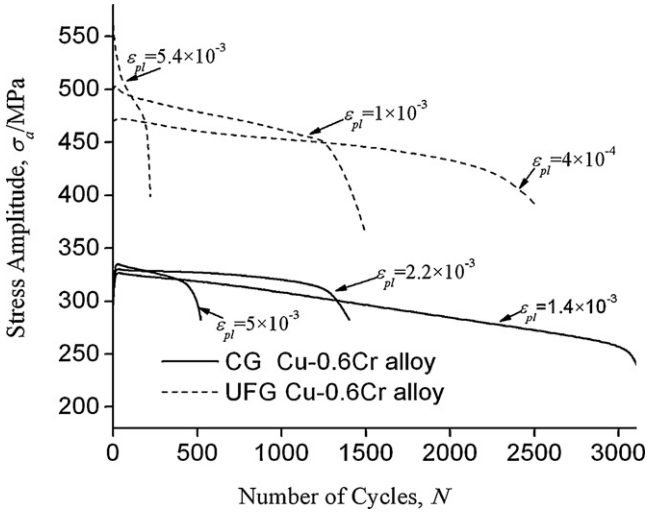

Fig. 6. Cyclic softening/hardening curves of the UFG and CG Cu–Cr alloy under the different plastic strain amplitude.

component is dominant and the fatigue life is determined by ductility. The explanation of this lifetime shortening behavior mainly lies in the low thermal and mechanical stability and a strong tendency to recover the severely plastic deformed UFG structure. In the literatures [24–27], cyclic softening, grain coarsening and strain localization appear to be the main mechanisms responsible for the lower fatigue resistance of UFG structures under the same plastic strain amplitude. The formation of shear bands with characteristic distributions of the defects formed during the last ECAP passes will lead to early crack nucleation and premature fatigue failure.

The cyclic stress response curves, which were determined by monitoring the stress response during total-strain-controlled fatigue, provide useful information pertaining to the mechanical stability of a material. As shown in Fig. 6, there is rapid cyclic hardening in early stage of cyclic deformation under different plastic strain amplitudes for CG samples, which is commonly associated with the formation of the vein dislocation structure in copper matrix during the cyclic deformation. The ECAP samples cyclically soften continuously before failure. Softening is particularly pronounced on the early stage of cycling. Cyclic softening, which is generally observed in cold worked metals, is related to the reduction in dislocation density. It has been recognized that ECAP

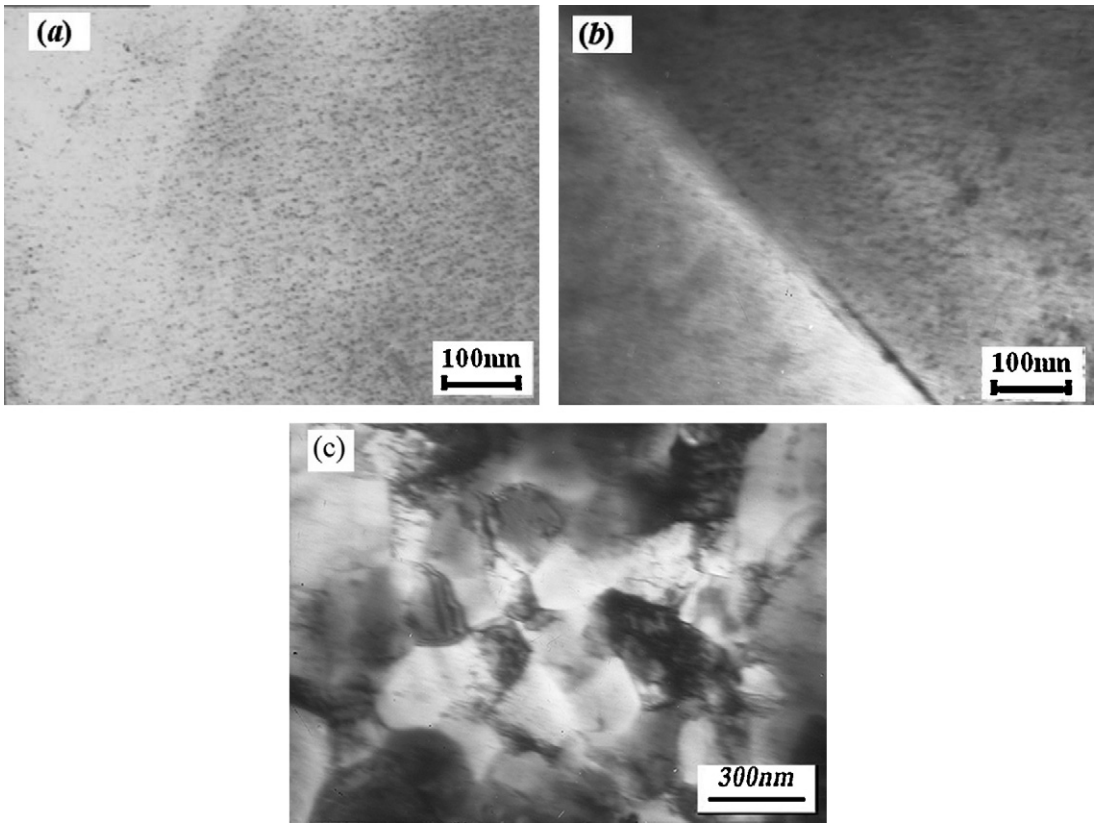

Fig. 7. TEM images of the structure of the Cu–Cr alloy: (a) CG alloy after aging at 753 K, (b) CG Cu–Cr alloy fatigued at $\varepsilon_{pl} = 5 \times 10^{-3}$, and (c) 12 passes ECAPed Cu–Cr alloy and fatigued at $\varepsilon_{pl} = 5 \times 10^{-3}$.

materials may soften to various degrees under cyclic loading. The rate of softening depends strongly on the initial structure and loading conditions and may vary in a wide range. Because the dislocation density is high as shown in Fig. 2(d), it is natural that the ECAP samples soften significantly. The UFG microstructure is supposed to trigger a very early crack formation due to a lack of ductility, as it is also indicated by the cyclic deformation curves. The softening degree markedly depends on the cyclic strain amplitude, the higher amplitude, the faster softening happens. From Fig. 6, it can be seen that the sample undergoing cyclic deformation with the highest plastic strain amplitude has the highest softening rate.

Fig. 7(a) and (b) shows a typical precipitate TEM micrograph of CG Cu–Cr alloy before and after cycling $\varepsilon_{pl} = 5 \times 10^{-3}$. The fine chromium precipitates (of 5–20 nm size) become visible in the copper matrix. In the present work, TEM does not reveal any significant difference in structure and the fraction, size of precipitated phase before and after cycling for CG Cu–Cr alloy aging at 753 K. Fig. 7(c) shows the microstructure of 12 passes ECAPed UFG Cu–Cr alloy after cycling at $\varepsilon_{pl} = 5 \times 10^{-3}$. Comparison of microstructural characteristics of UFG Cu–Cr alloy before (Fig. 2(d)) and after fatigue (Fig. 7(c)), show that the dislocation recovery occurs by annihilation in the grain body and the low-angle boundaries can disappear by repeated to and fro movement of dislocations. Thereby the total dislocation density reduces and constrains for dislocation motion removes. It is all much difficult to observe fine precipitates in the grain interior even at high magnifications for UFG Cu–Cr alloy before and after fatigue. UFG Cu–Cr alloy does not exhibit visible grain coarsening after fatigue.

As we know, the dense network of dislocations is one of the most important strengthening mechanisms for the UFG materials processed by ECAP [28,29]. Thus, one can conclude that cyclic softening of UFG Cu–Cr alloy is associated with some dislocation annihilation and the substructure recovery during cyclic deformation as a result of the to-and-fro motion of the dislocations. We should underline that the dislocations annihilation becomes easier and the rate of softening increases when the plastic strain amplitude increases.

Since the starting point of fatigue failure usually occurs at the metal surface, clarifying the mechanism of surface damage formation is important to understand the fatigue characteristics of UFG metals. To investigate the surface damage, the development of shear bands (SBs) on the surface of the cycled UFG Cu–Cr alloy was observed under all strain amplitudes. The density of SBs was higher as strain amplitude increased. As shown in Fig. 8 the SBs formed under plastic strain amplitude $\varepsilon_{pl} = 5 \times 10^{-3}$, which were approximately parallel to the shearing plane of last pressing and were oriented at about 45° and 90° with respect to the loading axis on XOZ plane and XOY plane, respectively. There is a difference in the density, length and mutual orientation of these bands on the two planes. On the XOZ plane, as shown in Fig. 8(a), where the traces of the last ECAP shear plane are parallel to the direction of the macroscopic maximum cyclic shear stress of the sample. They are long, parallel to each other and their density is higher than that on the XOY plane. On the XOY plane, as shown in Fig. 8(b), where the direction of maximum cyclic shear stress is perpendicular to the loading axis, the SBs are shorter and less developed. This result clearly indicates the important role of SBs in the fatigue crack initiation process. Some researchers recently attempted to explain SBs formation with relation to the oriented distribution of defects along the shear plane of the final pressing [30,31]. Furthermore, the studies indicate that damage often appears to be directly related to the instability of the UFG microstructures with a non-equilibrium state of grain boundaries (GBs). Fatigue-induced shear bands are considered to be one of the many possible causes of the cyclic softening observed. Cyclic softening in metals is usually associated with the ease of dislocation annihilation and is inherited from plastic prestraining. At a later stage, other morphology of protrusions with the different orientations from the shear direction of the last pressing was formed. The alternating extrusions and intrusions can be clearly seen together with cracks connecting the most developed bands. The final fatigue crack develops by connecting of parallel cracked bands.

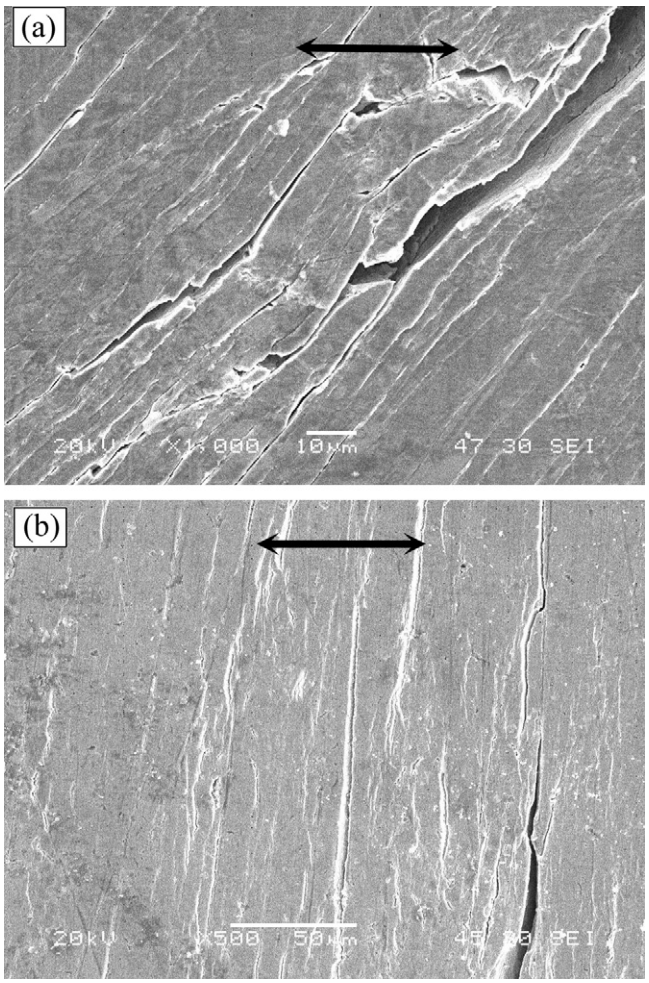

Fig. 8. Surface morphology of sample after strain-controlled cyclic deformation under $\varepsilon_{pl} = 5 \times 10^{-3}$: (a) XOZ plane and (b) XOY plane (the arrows show the loading direction).

As a matter of fact, residual macrostresses may have a profound effect on fatigue crack. Since fatigue cracks normally initiate at the surface, surface residual stresses are crucial to crack initiation and early stages of crack propagation. Apparently ECAP gives rise to high residual stresses across the samples. However, their magnitude and distribution still need to be studied in the other properties of interest.

4. Conclusion

Ultrafine grained Cu–Cr produced by ECAP was tested for investigating mechanical properties and fatigue behavior, including cyclic softening and fracture surface morphology. The following conclusions can be drawn:

(1) The average grain size of Cu–Cr alloy was refined to about 230 nm by ECAP for 12 passes and the alloy possesses high strength and sufficient ductility.

(2) The ECAPed samples under strain controlled fatigue exhibit lower fatigue limit because of the lower ductility of the UFG material, compared to the CG Cu. The UFG samples under strain-controlled loading show rapid cyclic softening, which occurs under all applied plastic strain amplitudes in early stage of testing.
(3) That cyclic softening of UFG Cu–Cr alloy is associated with some dislocation annihilation and the substructure recovery during cyclic deformation as a result of the to-and-fro motion of the dislocations. The dislocations annihilation become easier and the rate of softening increase when the plastic strain amplitude increases.
(4) The shear bands on the surface of cycled samples of UFG Cu–Cr alloy were investigated by scanning electron microscopy. It is shown that shear bands, microcracks and final fracture occur predominantly along the shear plane corresponding to the last ECAP.

Acknowledgements

This work was supported by the National Natural Science Foundation of China (Grant No. 51104113) and Scientific Research Program Funded by Shaanxi Provincial Education Department (Program No. 2010JK650).

References

[1] F. Rubitschek, T. Niendorf, I. Karaman, H.J. Maier, J. Alloys Compd. 517 (2012) 61–68.
[2] S.N. Alhajeri, N. Gao, T.G. Langdon, Mater. Sci. Eng. A 528 (2011) 3833–3840.
[3] Y. Iwahashi, Z. Horita, M. Nemoto, T.G. Langdon, Acta. Mater. 46 (1998) 3317–3331.
[4] R.Z. Valiev, Nat. Mater. 3 (2004) 511–516.
[5] M.S. Soliman, E.A. El-Danaf, A.A. Almajid, Mater. Sci. Eng. A 532 (2012) 120–129.
[6] K.R. Cardoso, D.N. Travessa, W.J. Botta, A.M. Jorge Jr., Mater. Sci. Eng. A 528 (2011) 5804–5811.
[7] K. Nakashima, Z. Horita, M. Nemoto, T.G. Langdon, Acta. Mater. 46 (1998) 1589–1599.
[8] A. Czerwinski, R. Lapovok, D. Tomus, Y. Estrin, A. Vinogradov, J. Alloys Compd. 509 (2011) 2709–2715.
[9] D.P. Delo, S.L. Semiatin, Metall. Mater. Trans. 30A (1999) 1391–1402.
[10] T.G. Langdon, Mater. Sci. Eng. A 462 (2007) 3–11.
[11] K. Neishi, Z. Horita, T.G. Langdon, Mater. Sci. Eng. A 352 (2003) 129–135.
[12] J.T. Wang, Z.Z. Du, F. Kang, Mater. Sci. Forum 503–504 (2006) 663–668.
[13] A. Vinogradov, A. Washikita, K. Kitagawa, V.I. Kopylov, Mater. Sci. Eng. A 349 (2003) 318–326.
[14] L. Kunz, P. Lukáš, M. Svoboda, Mater. Sci. Eng. A 424 (2006) 97–104.
[15] H. Mughrabi, H.W. Höppel, Int. J. Fatigue 32 (2010) 1413–1427.
[16] A. Vinogradov, V. Patlan, Y. Suzuki, K. Kitagawa, V.I. Kopylov, Acta Metall. 50 (2002) 1636–1651.
[17] A. Vinogradov, T. Ishida, K. Kitagawa, V.I. Kopylov, Acta Mater. 53 (2005) 2181–2192.
[18] P.S. De, R.S. Mishra, Mater. Sci. Eng. A 527 (2010) 7719–7730.
[19] D.M. Zhao, Q.M. Dong, P. Liu, Mater. Chem. Phys. 79 (2003) 81–86.
[20] C.Z. Xu, Q.J. Wang, M.S. Zheng, et al., Mater. Sci. Eng. A 459 (2007) 303–308.
[21] M. Furukawa, Y. Iwahashi, Z. Horita, M. Nemoto, T.G. Langdon, Mater. Sci. Eng. A 257 (1998) 328–332.
[22] R.Z. Valiev, A.V. Korznikov, R.R. Mulyukov, Mater. Sci. Eng. A 168 (1993) 141–148.
[23] T. Liu, W. Zhang, S.D. Wu, C.B. Jiang, S.X. Li, Y.B. Xu, Mater. Sci. Eng. A 360 (2003) 345–349.
[24] S. Suresh, Fatigue of Materials, Cambridge University Press, UK, 1998, p. P617.
[25] H.J. Maier, P. Gabor, I. Karaman, Mater. Sci. Eng. A 410–411 (2005) 457–461.
[26] S.R. Agnew, J.R. Weertman, Mater. Sci. Eng. A 244 (1998) 145–153.
[27] S.D. Wu, Z.G. Wang, C.B. Jiang, G.Y. Li, I.V. Alexandrov, R.Z. Valiev, Scripta Mater. 48 (2003) 1605–1609.
[28] R.Z. Valiev, T.G. Langdon, Prog. Mater. Sci. 51 (2006) 881–981.
[29] A. Vinogradov, S. Hashimoto, Mater. Trans. 42 (2001) 74–84.
[30] M. Goto, S.Z. Han, T. Yakushiji, C.Y. Lim, S.S. Kim, Scripta Mater. 54 (2006) 2101–2106.
[31] M. Goto, S.Z. Han, S.S. Kim, N. Kawagoishi, C.Y. Lim, Scripta Mater. 57 (2007) 293–296.